The evolution of a Milky Way-like galaxy in a cosmological context

E. Colavitti[a], F. Matteucci[a,b] and G. Murante[c]
[a]Dipartimento di Astronomia, Università di Trieste, via G. B. Tiepolo 11, 34131 Trieste (TS), Italy
[b] I.N.A.F. Osservatorio Astronomico di Trieste, via G. B. Tiepolo 11, 34131 Trieste (TS), Italy
[c] I.N.A.F. Osservatorio Astronomico di Torino, via Osservatorio 20, 10025 Pino Torinese (TO), Italy

Abstract
We test several gas infall laws, starting from that suggested in the two-infall model for the chemical evolution of the Milky Way, but focusing on laws derived from cosmological simulations which follows a concordance ΛCDM cosmology. By means of a detailed chemical evolution model we study the effects of the different gas infall laws on the abundance patterns and the G-dwarf metallicity distribution. One cosmological gas infall law in particular resembles the infall law suggested by the two-infall model. It predicts two main gas accretion episodes. Minor infall episodes are predicted to have followed the second main one but they are of little significance compared to the previous two. By means of this cosmologically motivated infall law, we study the star formation rate, the SNIa and SNII rate, the total amount of gas and stars and the behavior of several chemical abundances. We find that the results of the two-infall model are fully compatible with the evolution of the Milky Way with cosmological accretion laws.

Introduction
Here we study the infall law that arises directly from the DM halo, testing it in a detailed model of chemical evolution of the Milky Way which follows the evolution of many chemical species by taking into account the stellar lifetimes, detailed nucleosynthesis prescriptions and the supernova (type II, Ib/c and Ia) rates. Several authors before us have tried to build a model for the evolution of disk galaxies in a cosmological context, but none of these considered the chemical evolution in such detail as our model. Naab & Ostriker (2006) studied the metallicity and photometric evolution of a generic disk galaxy by assuming that it forms through mergers of dark matter halos. They concluded that the infall rate should have been almost constant during the lifetime of the disk. However no detailed chemical evolution was followed. We compare the chemical results with those of François et al.'s (2004) model. For the single stars in the mass range $0.8\ M_\odot \leq M \leq 8\ M_\odot$ we adopt here the stellar yields of van den Hoek & Groenewegen (1997). For SNIa we adopt the single-degenerate progenitor scenario (Whelan & Iben, 1973; Han & Podsiadlowski 2004) and we assume the stellar yields from Iwamoto et al. (1999). For massive stars ($8\ M_\odot < M \leq 100\ M_\odot$) we adopt the stellar yields by Woosley & Weaver (1995) with the suggested modifications of François et al. (2004). We start with primordial gas. The reference solar abundances are those by Asplund et al. (2005).
The model by Chiappini et al. (1997) was the first in which two main infall episodes for the formation of the Galactic components were suggested. They assumed that the first infall episode was responsible for the formation of the halo and thick-disk stars. The second infall episode formed the thin-disk component, with a timescale much longer than that of the thick-disk formation. The authors also included in the model a threshold in the gas density below which the star formation process stops. With these precise prescriptions it is possible to reproduce the majority of the observed properties of the Milky Way. In the model by Chiappini et al. (1997) the Galactic disk is approximated by a series of concentric annuli, 2 kpc wide, without exchange of matter between them. The basic equations are the same as in Matteucci & François (1989). The two models have in common the "inside-out" formation of the thin disk. The SFR is a Schmidt (1955) law with a dependence on the surface gas density and also on the total surface mass density. The IMF is that of Scalo (1986) normalized over a mass range of 0.1-100 $M_\odot$ and it is assumed to be constant in space and time.

The cosmological simulation
We run a dark matter-only cosmological simulation, using the public tree-code GADGET2 (Springel 2005), in order to produce and study dark matter halos in which spiral galaxies can form. Our simulated box has a side of 24 h^{-1} Mpc. We used 256^3 particles. We adopted the standard cosmological parameters from WMAP 3-years (Spergel et al. 2007), namely $\Omega_0 = 0.275$, $\Omega_\lambda = 0.725$ and $\Omega_b = 0.041$. Each DM particle has a mass equal to $6.289 \cdot 10^7 h^{-1} M_\odot$ and the Plummer-equivalent softening length is set to 3.75 h^{-1} comoving kpc to redshift $z = 2$ and to $1.25\, h^{-1}$ physical kpc since $z = 2$. We use the public package GRAFIC (Bertschinger 1995) to set up our initial conditions. The simulation started at redshift $z = 20$. We checked that the final mass function of DM halos and the power spectrum are in agreement with theoretical expectations.

To identify the DM halos that can host a spiral galaxy similar to the MW we used selection criteria based on four different characteristics of the halos:

- mass between $5 \cdot 10^{11} M_\odot$ and $5 \cdot 10^{12} M_\odot$;
- spin parameter $\lambda > 0.04$;
- redshift of last major merger larger than $z = 2.5$;
- redshift of formation larger than $z = 1.0$.

We found four DM halos compatible with our selection criteria. We label them with their F-o-F group number, i.e. group 48001, group 52888, group 56004 and group 6460. We note that, given our simulated volume, the expected number of halos in our mass range is higher: using a Press & Schechter mass function, approximately 70 halos are expected.
However, the requirement of having a "quiescent" formation history and a high spin parameter greatly reduces their number. We assumed that the derived infall law has the same functional form for the whole Milky Way, but that the normalization constant is different for different Galactic regions. In other words, the normalization constants were obtained by reproducing the current total surface mass density at any specific galactocentric distance, although here we will focus on the solar neighbourhood. Finally, we also considered the arithmetic mean of the infall laws of all four halos, in order to have an "average" cosmological infall law to study. In Table 1 we summarize the characteristics of the halos.

Table 1 Characteristics of the DM halos.

Group	Mass [$10^{10} M_\odot$]	Spin parameter	Redshift major merger	Redshift of formation
48001	90.26	0.045	5.00	1.75 - 1.50
52888	465.75	0.059	3.75	1.50 - 1.25
56009	90.73	0.049	3.25	2.00 - 1.75
6460	61.94	0.041	2.50	1.25 - 1.00

The infall laws
In testing the accretion laws, we started by adopting the two-infall law model, as suggested by Chiappini et al. (1997) (Model 1). Besides this infall law, we tested other possible laws, such as a time constant infall rate (Model 2), a linear infall law (Model 3) and an infall law that is the same as that of Chiappini et al. (1997) but with pre-enriched infalling gas (Model 4).
Then we tested the cosmological infall laws. To derive the cosmological infall law we proceeded in the following way:

$$A(r,t) = a(r) 0.19 \frac{dM_{DM}}{dt} [M_\odot\ pc^{-2}\ Gyr^{-1}]. \quad (1)$$

where 0.19 is the cosmological baryonic fraction and $a(r)$ is a normalization constant fixed to reproduce the current total surface mass density along the disk. For the solar ring $a(r) = \frac{\Sigma(r_\odot, t_G)}{M_{Gal}}$, with $M_{Gal} = 0.19 M_{DM}$ being the baryonic mass of our Galaxy and t_G the Galactic lifetime.
One infall law is given by the arithmetic average of the infall laws derived for the four halos and the last infall law is that suggested by Naab & Ostriker (2006). Our infall laws for the solar region are shown in Figure 1 (left panel). Every figure has the same characteristics. Upper left panel: red solid line is the two-infall model (Model 1); black dashed line is the cosmological mean model (Model 9); green dotted line is the model by Naab & Ostriker (2006) (Model 10). Upper right panel: magenta solid line is the constant infall model (Model 2); blue dashed line is the linear infall model (Model 3); cyan dotted line is the pre-enriched model ($Z_{inf} = 1/10\ Z_{today}$, Model 4). Bottom left panel: black solid line is Model 5; magenta dashed line is Model 6. Bottom right panel: blue solid line is Model 7; cyan dashed line is Model 8. The assembly history of our best halo (Model 5) presents two distinct accretion peaks which produce an infall law very similar to the two-infall model by Chiappini et al. (1997), even if the two peaks are placed at a lower redshifts. In Fig. 1, right panel, we present the total surface mass density Σ_{tot}, expressed as $M_\odot pc^{-2}$, as a function of time for all the models.

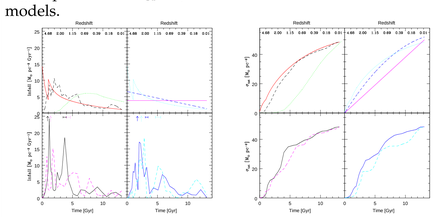

Figure 1 Left panel: Infall vs time; Right panel: Σ_{tot} vs time

Models 1 and 4 have the same Σ_{tot}. The linear model predicts the largest final amount of matter. The constant model has a linear growth. Model 10 is the only one that starts to increase the amount of matter very slowly (in the solar neighbourhood). The cosmological models produce results that are quite similar to the two-infall model.

Results
In Fig. 2, left panel, we show the infall law derived from Model 5 (our best halo) for three galactocentric distances (4, 8 and 14 kpc).
Figure 2 (right panel) shows the star formation rate as a function of cosmic time for all the models. At high redshift there is a gap in the SFR for some of the models, due to the adoption of a threshold in the surface gas density. We deduce that the constant infall model predicts a growing star formation rate at low redshifts, a trend that is not predicted by the other laws. On the other hand, the cosmological best model predicts a very important peak between 3 and 6 Gyr, which should correspond to the formation of the bulk of the stars in the thin disk. After 10 Gyr from the Big Bang the threshold is easily reached in most of the models, thus causing the SFR to have an oscillating behaviour.

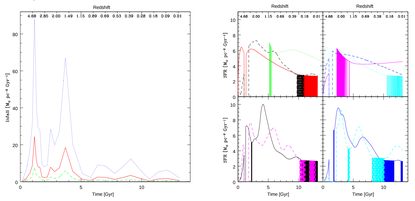

Figure 2 Left panel: infall law of our best cosmological halo at three different radii (4 kpc: blue dotted line; 8 kpc: red solid line; 14 kpc: green dashed line); Right panel: SFR vs time

In Figure 3 (left panel) we present the SNIa rates for all the models. The cosmological law of Model 5 predicts a peak for the SNIa rate at about 6 Gyr. This is due to the fact that the SFR in this model has a large peak at about 5 Gyr. Thanks to this peak, many stars form and many SNIa explode after a delay of about 1 Gyr. All the models predict a SNIa rate between 0.003 and 0.004 SNe $pc^{-2}\ Gyr^{-1}$, in good agreement with the value given by Boissier & Prantzos (1999), i.e. 0.0042 ± 0.0016 .
In Figure 3 (right panel) we present the predicted [Fe/H] as a function of time for all models. The model with a constant infall law and Model 10 never reach the solar abundance. The reason is that in both models the infall rate during the whole galactic lifetime is probably overestimated. In the model by Chiappini et al. (1997) [Fe/H] reaches a local peak at 1 Gyr, then decreases slightly to increase again. The small depression in [Fe/H] is due to the predicted gap in the SFR just before the formation of the thin disk. The second infall episode coupled with the halt in the SF produces a decrease of [Fe/H]. We can see the same behaviour in the cosmological models. In particular in Model 5 the peak is followed by a deeper depression of [Fe/H] and this is due to the longer gap in the SFR predicted by this model (1-2 Gyr) as opposed to that predicted by Model 1. This is an important prediction and it can be tested via chemical abundances. Both Gratton et al. (1996) and Furhmann (1998) detected such an effect in the [Fe/O] vs. [O/H] and [Fe/Mg] vs. [Mg/H], respectively.

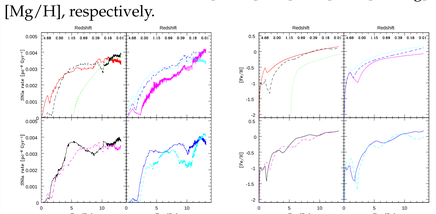

Figure 3 Left panel: SNIa vs time; Right panel: [Fe/H] vs time.

A very important constraint for the chemical evolution of the galaxies is represented by the G-dwarf metallicity distribution. This is the relative number of G-dwarf stars as a function of [Fe/H]. Our predicted metallicity distributions are shown in Figure 4, left panel. From this figure, it is clear that Model 10 predicts insufficient high metallicity stars. On the other hand, some of the cosmological models such as Model 7 and Model 8 predict too many metal-poor stars.

Our best cosmological model shows a bimodal metallicity distribution, which is clearly at odds with the data.
In Figure 4, right panel, we show the O abundance gradient as predicted by Model 1 and Model 5, compared with a compilation of data including Cepheids (see Cescutti et al. 2007). The O gradient predicted by Model 5 flattens for $r < 8$ kpc whereas it agrees very well with the slope predicted by Model 1 (the original two-infall model) for $r \geq 8$ kpc. Model 1 contains the assumption of an inside-out formation of the disk, whereas in Model 5 no such assumption is made. In spite of that, the two predicted gradients are similar and we cannot reject the O gradient predicted by Model 5 on the basis of the comparison with data. The reason for that probably resides in the adoption of the star formation threshold which acts mainly at large galactocentric distances where the gas density is lower. This effect predominates over the increase of the timescale for disk formation.

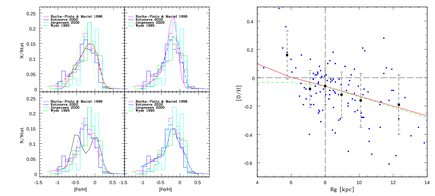

Figure 4 Left panel: G-dwarf metallicity distribution; Right panel: predicted and observed O abundance gradients in the galactocentric distance range 4 - 14 kpc.

In Figure 5 (left panel) the [O/Fe] as a function of [Fe/H] can be seen. Here, the range of [Fe/H] has been restricted to -2.0 to $+0.3$ dex in order to better see the predictions relative to the transition between the halo-thick disk and the thin disk.
In Figure 5 (right panel) we show the same plots but for the whole range of [Fe/H] down to -4.0 dex. The data are from: Cayrel et al. (2004) (red triangles) and François et al. (2004) (green crosses). One can see that cosmological models have a similar behaviour to the model by Chiappini et al. (1997), except for a longer gap in the SF, which produces a loop in the predicted curves. Such loops arise when SF stops, the α-elements are no longer produced whereas Fe continues to be produced.
This induces the [O/Fe] to decrease and also the [Fe/H] ratio to decrease to a lesser extent, because of the accretion of primordial gas. Then when SF starts again the [O/Fe] again increases. This loop is very prominant in some models and is not in agreement with the data, although some spread is present. Model 4, which is the same as Chiappini et al's model but with the pre-enriched gas, is acceptable. This is due to the fact that the metallicity of the pre-enriched infalling gas is not so different from the metallicity of the primordial infalling gas.

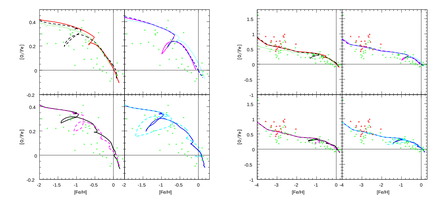

Figure 5 Left and right panels: [O/Fe] vs [Fe/H].

Conclusions
Our main conclusions can be summarized as follows:

- A model with constant infall predicts a present day infall rate and SFR larger than all the other models. Moreover, it is the only model that produced an unrealistically increasing SFR during the last billion years. This is probably an unrealistic law, and we only used it for comparison with other infall laws.
- The linear model predicts the largest number of stars presently in the solar neighbourhood but it seems to reproduce reasonably well all the other observables. However, this model does not describe the evolution of our Galaxy as well as an exponential law does.
- The model adopting the two-infall law, but where the gas is assumed to be pre-enriched during the formation of the disk at the level of 1/10 of solar, well reproduces the G-dwarf metallicity distribution, as expected.
- The cosmological laws, and in particular our preferred best fit, seem to fit well all the data. This law predicts two main accretion episodes which can be identified with the formation of the halo-thick disk and thin disk, respectively, very similar to the two-infall law. Moreover, there seems to be a gap of 1-2 Gyr in the SFR between the two episodes, larger than predicted by Chiappini et al. (1997) (< 1 Gyr). The gap is due mainly to the adoption of a threshold gas density for the star formation rate. The model including this cosmological infall law can well reproduce most of the observational constraints. It predicts for the G-dwarf metallicity distribution, in the solar vicinity, two different peaks: we speculate that the first peak represents the stars of the halo and thick disk while the second peak represents the stars of the thin disk. The same metallicity distribution computed for the central region should also include the bulge stars. The predicted timescales for the formation of the halo-thick disk and the thin disk, respectively, are in excellent agreement with those suggested by Chiappini et al. In particular, the halo-thick disk must have formed on a timescale not longer than 1-2 Gyr whereas the thin disk in the solar vicinity took at least 6 Gyr to assemble 60% of its mass. As a consequence of the gap between the halo-thick disk and the thin disk, we predict that the thin disk is at least 2 Gyr younger than the halo.
- The other cosmological infall laws are characterized by several minor accretion events after the two main ones and predict larger gaps in the SFR which are not observed in the [Fe/O] vs. [O/H] and [Fe/Mg] vs. [Mg/H] which indicate a gap not larger than 1-2 Gyr.
- A model adopting a cosmologically inferred infall law by Naab & Ostriker (2006) presents a behaviour very similar to the constant infall law and predicts too low metallicities at the Sun's age and at the present time. Moreover, this model predicts a too small number of G-dwarfs with high metallicity. In their paper they present a G-dwarf metallicity distribution but as a function of Z which represents O and not Fe, as in the observations.

References
[1] Asplund M., Grevesse N. & Sauval A. J., 2005, ASPC, 336, 25
[2] Bertschinger E., 1995, astro.ph, 6070
[3] Boissier S. & Prantzos N., 1999, MNRAS, 307, 857
[4] Carbon D. F., Barbuy B., Kraft R. P., Friel E. D. & Suntzeff N. B., 1987, PASP, 99, 335
[5] Cayrel R., Depagne E., Spite M., Hill V., Spite F., François P., Plez B., Beers T. et al., 2004, A&A, 416, 1117
[6] Cescutti G., Matteucci, F. François P. & Chiappini, C. 2007, A&A, 462, 943
[7] Chiappini C., Matteucci F. & Romano D., 2001, ApJ, 554, 1044
[8] François P., Matteucci F., Cayrel R., Spite M., Spite F. & Chiappini C., 2004, A&A, 421, 613
[9] Gratton R., Carretta E., Matteucci F. & Sneden C., 1996, ASPC, 92, 371
[10] Han Z. & Podsiadlowski P., 2004, MNRAS, 350, 1301
[11] Israelian G., Ecuvillo A., Rebolo R., García-López R., Bonifacio P. & Molaro P., 2004, A&A, 421, 649
[12] Iwamoto K., Brachwitz F., Nomoto K., Kishimoto N., Umeda H., Hix W. R. & Thielemann F. K., 1999, ApJS, 125, 439
[13] Jørgensen B. R., 2000, A&A, 363, 947
[14] Kotoneva E., Flynn, C., Chiappini, C. & Matteucci, F., 2002, MNRAS 336, 879
[15] Laird J. B., 1985, ApJS, 57, 389
[16] Matteucci F. & François P., 1989, MNRAS, 239, 885
[17] Naab T. & Ostriker J. P., 2006, MNRAS, 366, 899
[18] Rocha-Pinto H. J. & Maciel W. J., 1996, MNRAS, 279, 447
[19] Scalo J. M., 1986, FCPh, 11, 1
[20] Spergel D. N., Bean R., Dor O., Nolta M. R., Bennet C. L., Dunkley J., Hinshaw J., Jarosik N. et al., 2007, ApJS, 170, 377
[21] Springel V., 2005, MNRAS, 364, 1105
[22] Tomkin J., Woolf V. M., Lambert D. L. & Lemke M., 1995, AJ, 109, 2204
[23] van den Hoek L. B. & Groenewegen M. A. T., 1997, A&AS, 123, 305
[24] Whelan J. & Iben I. Jr., 1973, ApJ, 186, 1007
[25] Woosley S. E. & Weaver T. A., 1995, AIPC, 327, 365